

Supplementary Information

Coupled-substitution on double-layer Aurivillius niobates:
Structure, magnetism and solar photocatalysis

Sonia Rani,^a Gollapally Naresh^{a,b} and Tapas Kumar Mandal*,^a

^a*Department of Chemistry, Indian Institute of Technology Roorkee, Roorkee 247667, India.*

^b*Department of Chemical and Biological Engineering, University of Sheffield, Sheffield, UK.*

E-mail: tapasfcy@iitr.ac.in

Table S1 Bond types and bond lengths of $\text{LaBi}_2\text{Nb}_{1.5}\text{M}_{0.5}\text{O}_9$ ($\text{M} = \text{Cr}, \text{Mn}, \text{Fe}, \text{Co}$)

Bond type	Bond lengths (\AA)			
	Cr	Mn	Fe	Co
M/Nb-O ₁	2.219(2)	2.187(1)	2.238(1)	2.242(1)
M/Nb-O ₂	1.885(1)	1.818(2)	1.857(3)	1.844(2)
M/Nb-O ₄	1.906(1)	1.890(2)	1.889(2)	1.935(2)
M/Nb-O ₄	2.120(3)	2.088(1)	2.161(1)	2.071(1)
M/Nb-O ₅	1.888(2)	1.837(2)	1.865(3)	1.826(2)
M/Nb-O ₅	2.056(2)	2.170(3)	2.077(2)	2.186(3)
Bi-O ₃	2.263(1)	2.227(2)	2.288(1)	2.218(1)
Bi-O ₃	2.279(2)	2.241(3)	2.272(2)	2.242(2)
Bi-O ₃	2.324(1)	2.343(1)	2.343(3)	2.376(1)
Bi-O ₃	2.403(1)	2.420(1)	2.419(2)	2.425(2)

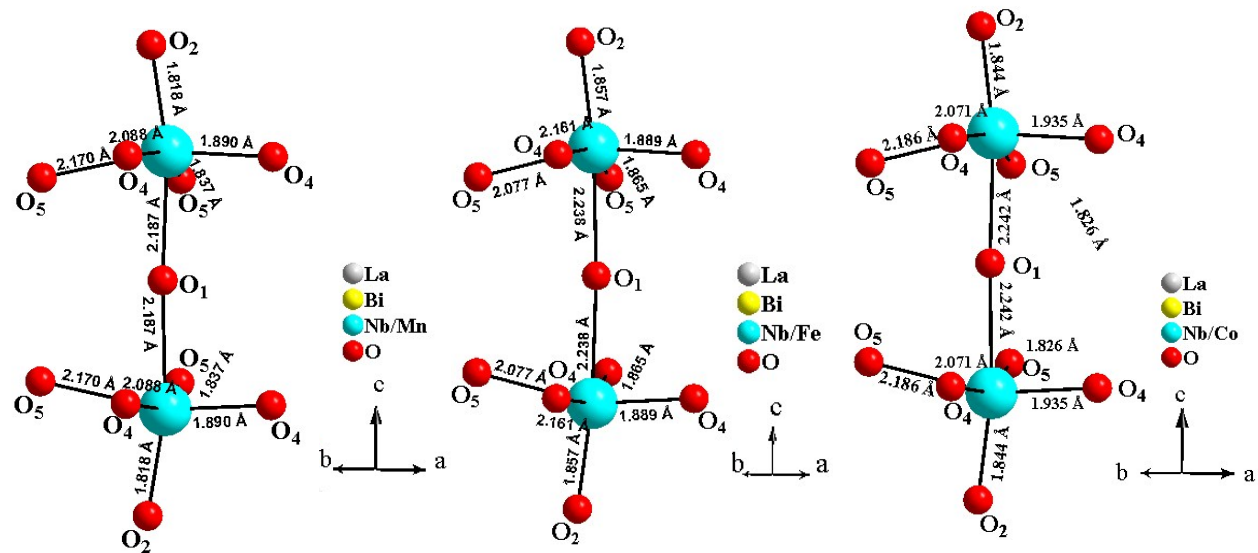


Fig. S1 Octahedral coordination environment of the double layer perovskite block for LaBi₂Nb_{1.5}M_{0.5}O₉ (M = Mn, Fe, Co).

Table S2 Octahedral distortion parameters, average axial, average equatorial and difference

Compounds	Octahedral distortion parameter (Δ_o)	Average axial bond distance ($d_{avg}^{ax}/\text{\AA}$)	Average equatorial bond distance ($d_{avg}^{eq}/\text{\AA}$)	Difference ($d_{avg}^{ax}) - (d_{avg}^{eq})$
LaBi ₂ Nb _{1.5} Cr _{0.5} O ₉	0.0244	2.0520	1.9925	0.0595
LaBi ₂ Nb _{1.5} Mn _{0.5} O ₉	0.0359	2.0025	1.9962	0.0063
LaBi ₂ Nb _{1.5} Fe _{0.5} O ₉	0.0340	2.0475	1.9980	0.0495
LaBi ₂ Nb _{1.5} Co _{0.5} O ₉	0.0381	2.0430	2.0045	0.0385

bond distances for LaBi₂Nb_{1.5}M_{0.5}O₉ (M = Cr, Mn, Fe, Co)

Calculation of octahedral distortion parameter (Δ_o) and average axial (d_{avg}^{ax}) and average equatorial (d_{avg}^{eq}) bond distances:

The octahedral distortion parameter (Δ_o), is defined as

$$\Delta_o = \frac{1}{6} \sum_{i=1}^6 [(l_i - \bar{l})/\bar{l}]^2$$

where, l_i = M–O bond distances present in an octahedra, \bar{l} = average M–O bond distance of the octahedra. The average axial and equatorial bond distances are calculated by taking the average of the axial and equatorial bonds, respectively, present in an octahedra.

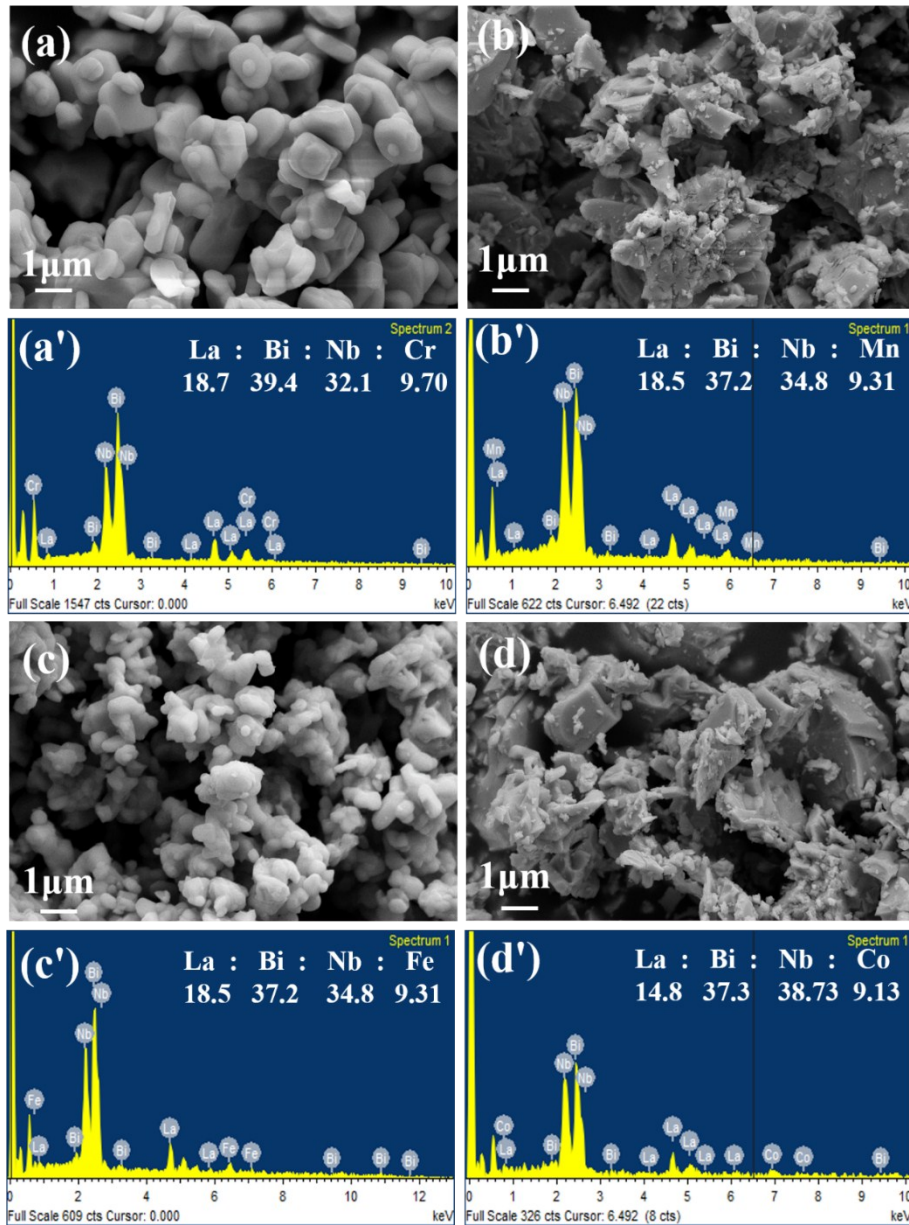


Fig. S2 FE-SEM image and corresponding EDX spectra of (a) & (a') LaBi₂Nb_{1.5}Cr_{0.5}O₉, (b) & (b') LaBi₂Nb_{1.5}Mn_{0.5}O₉, (c) & (c') LaBi₂Nb_{1.5}Fe_{0.5}O₉, and (d) & (d') LaBi₂Nb_{1.5}Co_{0.5}O₉.

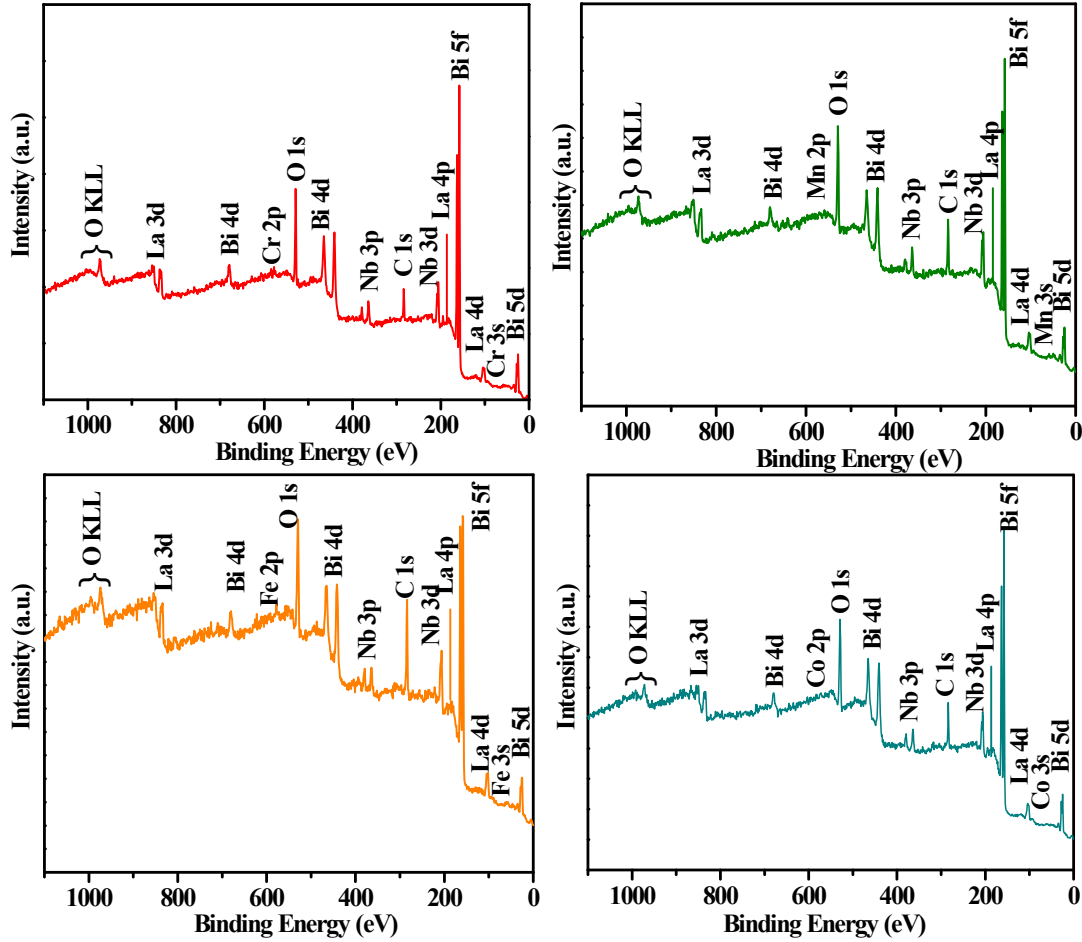


Fig. S3 Survey XPS for $\text{LaBi}_2\text{Nb}_{1.5}\text{M}_{0.5}\text{O}_9$ ($\text{M} = \text{Cr}, \text{Mn}, \text{Fe}$ and Co).

Table S3 Observed and calculated magnetic moments, band gaps and band edge energies for $\text{LaBi}_2\text{Nb}_{1.5}\text{M}_{0.5}\text{O}_9$ ($\text{M} = \text{Cr}, \text{Mn}, \text{Fe}, \text{Co}$)

Compounds	μ_{obs} (BM)	$\mu_{\text{spin-only}}$ (BM)	Band gap and band edge energies (eV)		
			E_g	$E_{\text{edge}} (1)$	$E_{\text{edge}} (2)$
$\text{SrBi}_2\text{Nb}_2\text{O}_9$	---	---	3.42	---	---
$\text{LaBi}_2\text{Nb}_{1.5}\text{Cr}_{0.5}\text{O}_9$	3.8	3.9	2.25	2.63	3.53
$\text{LaBi}_2\text{Nb}_{1.5}\text{Mn}_{0.5}\text{O}_9$	3.6	4.9 (HS)	2.94	3.45	---
$\text{LaBi}_2\text{Nb}_{1.5}\text{Fe}_{0.5}\text{O}_9$	5.3	5.9 (HS)	2.37	2.73	3.47
$\text{LaBi}_2\text{Nb}_{1.5}\text{Co}_{0.5}\text{O}_9$	5.1	4.9 (HS)	2.29	2.62	3.48

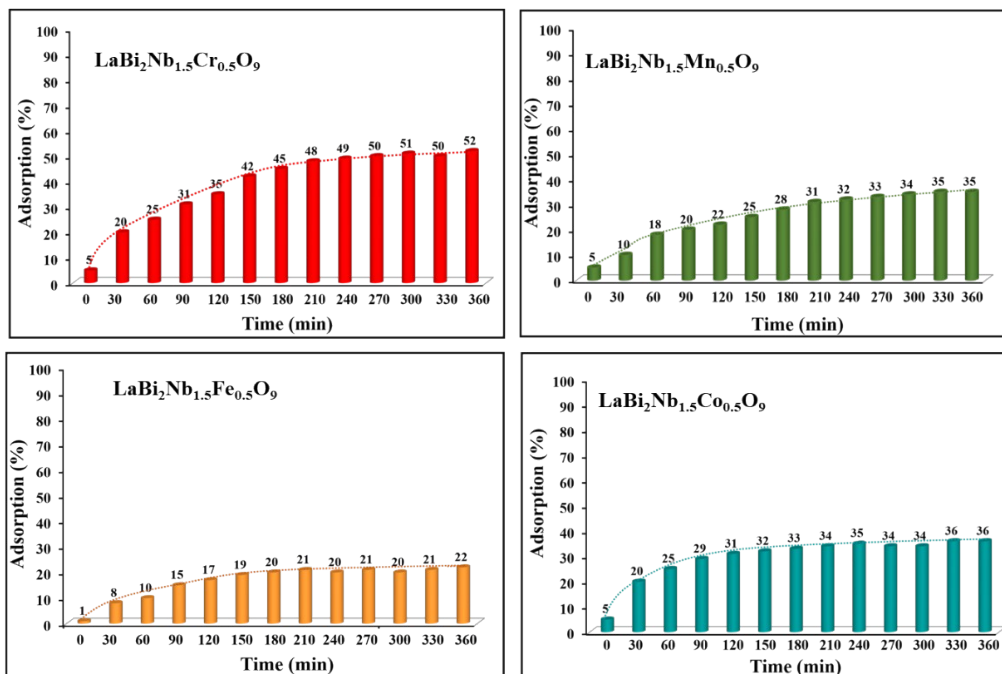


Fig. S4 Adsorption profiles with time for $\text{LaBi}_2\text{Nb}_{1.5}\text{M}_{0.5}\text{O}_9$ ($\text{M} = \text{Cr}, \text{Mn}, \text{Fe}$ and Co).

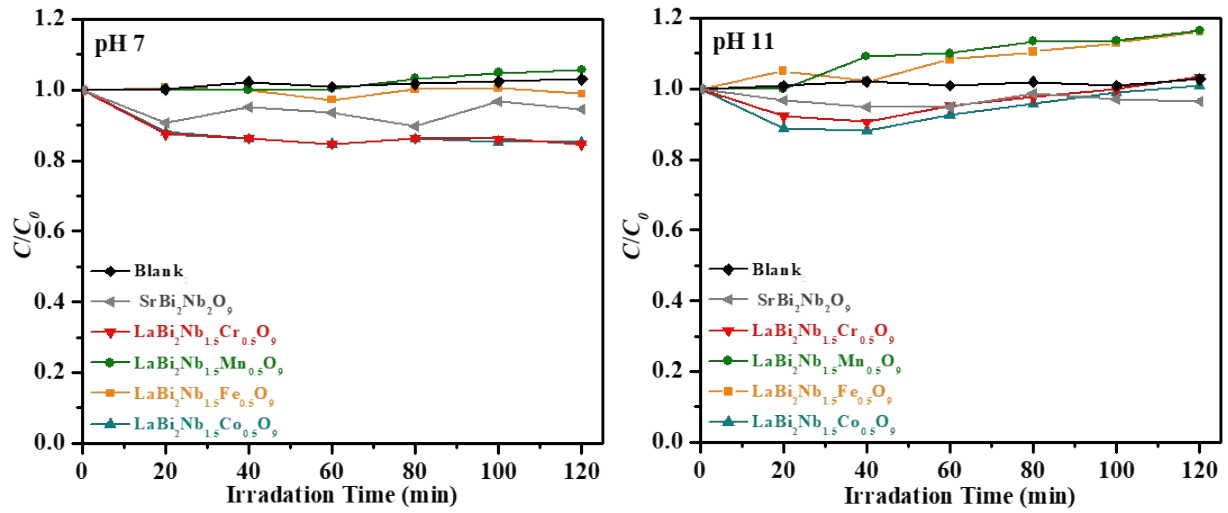


Fig. S5 RhB degradation over $\text{LaBi}_2\text{Nb}_{1.5}\text{M}_{0.5}\text{O}_9$ ($\text{M} = \text{Cr}, \text{Mn}, \text{Fe}$ and Co) at pH 7 and 11.

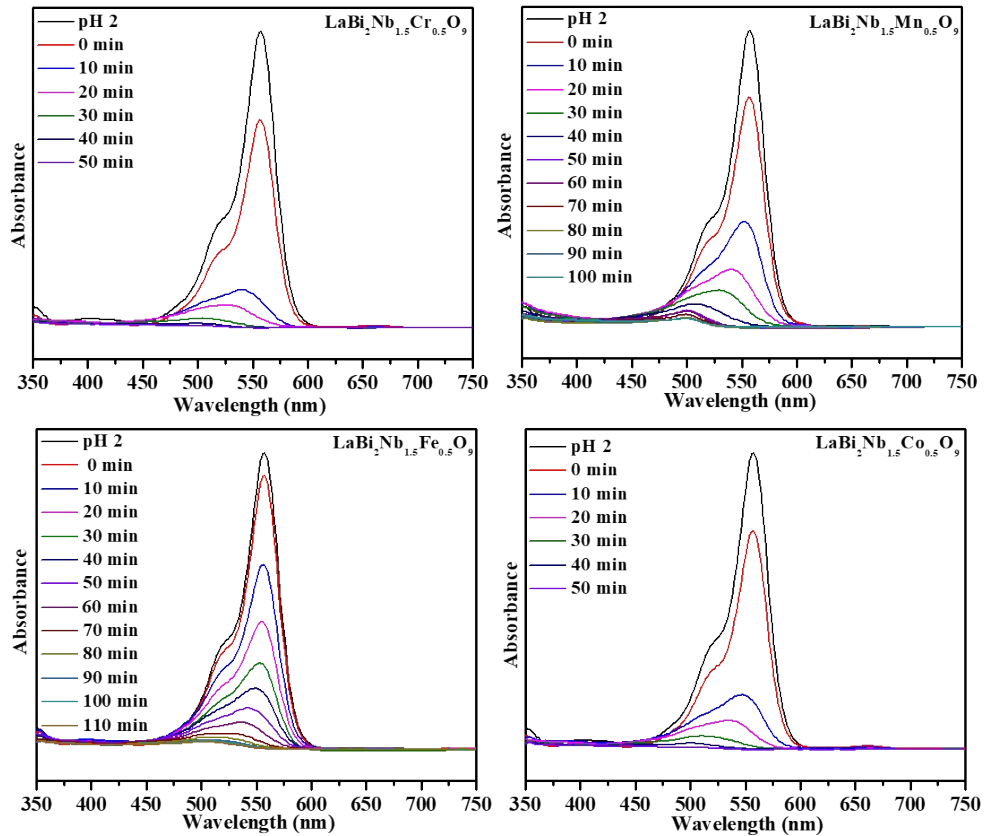


Fig. S6 Absorption profiles of RhB degradation over $\text{LaBi}_2\text{Nb}_{1.5}\text{M}_{0.5}\text{O}_9$ ($\text{M} = \text{Cr}, \text{Mn}, \text{Fe}, \text{Co}$) at pH 2 under solar irradiation.

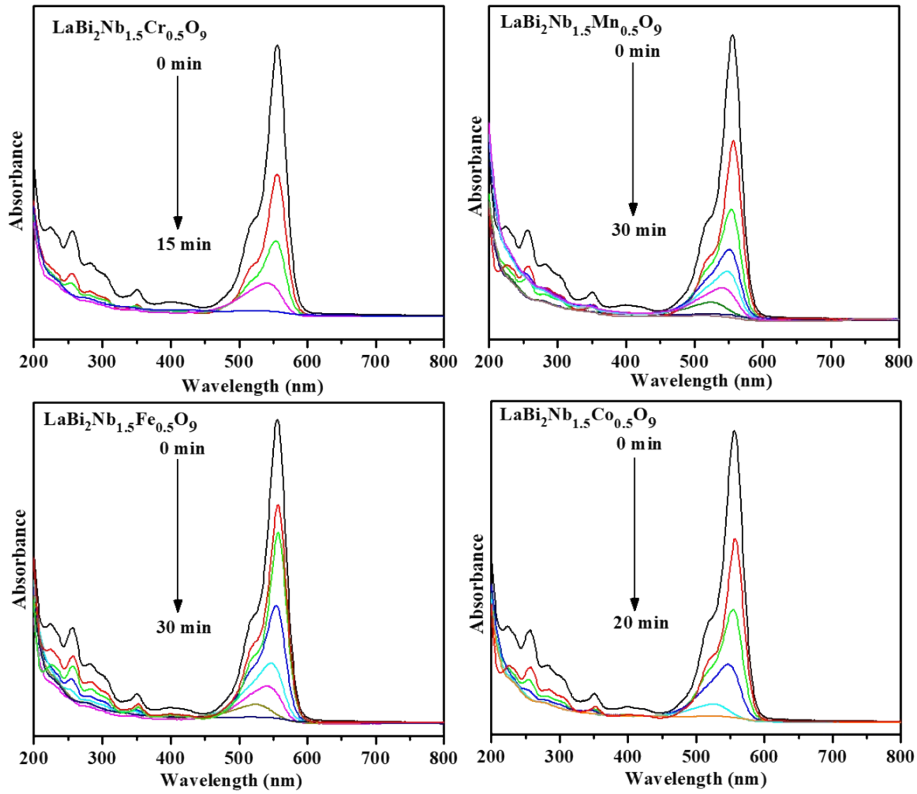


Fig. S7 UV-vis absorbance data for RhB degradation over $\text{LaBi}_2\text{Nb}_{1.5}\text{M}_{0.5}\text{O}_9$, ($\text{M} = \text{Cr}, \text{Mn}, \text{Fe}$ and Co) at pH 2 under medium pressure mercury vapour lamp (UV-visible light).

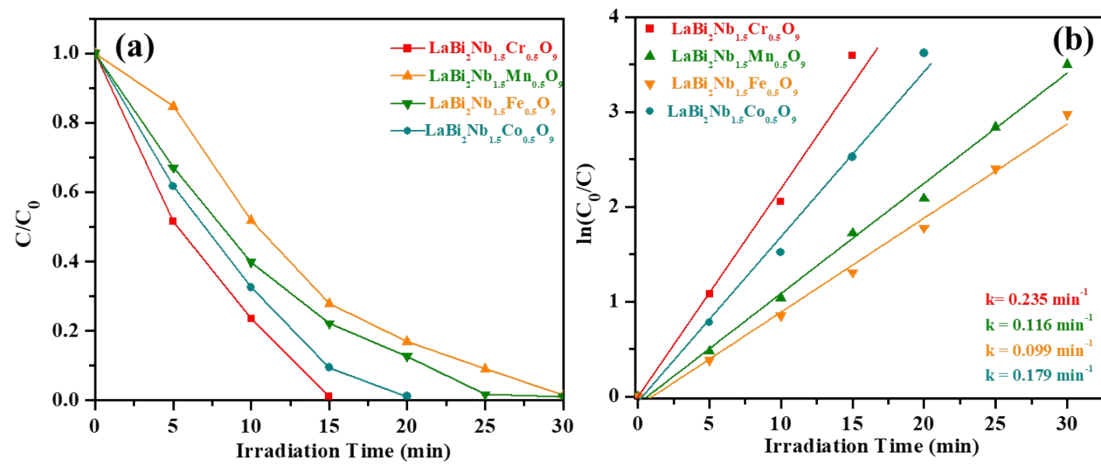


Fig. S8 (a) C/C_0 and (b) $\ln(C_0/C)$ as a function of irradiation time (min) for RhB degradation over $\text{LaBi}_2\text{Nb}_{1.5}\text{M}_{0.5}\text{O}_9$, ($\text{M} = \text{Cr}, \text{Mn}, \text{Fe}$ and Co) at pH 2 under medium pressure mercury vapour lamp.

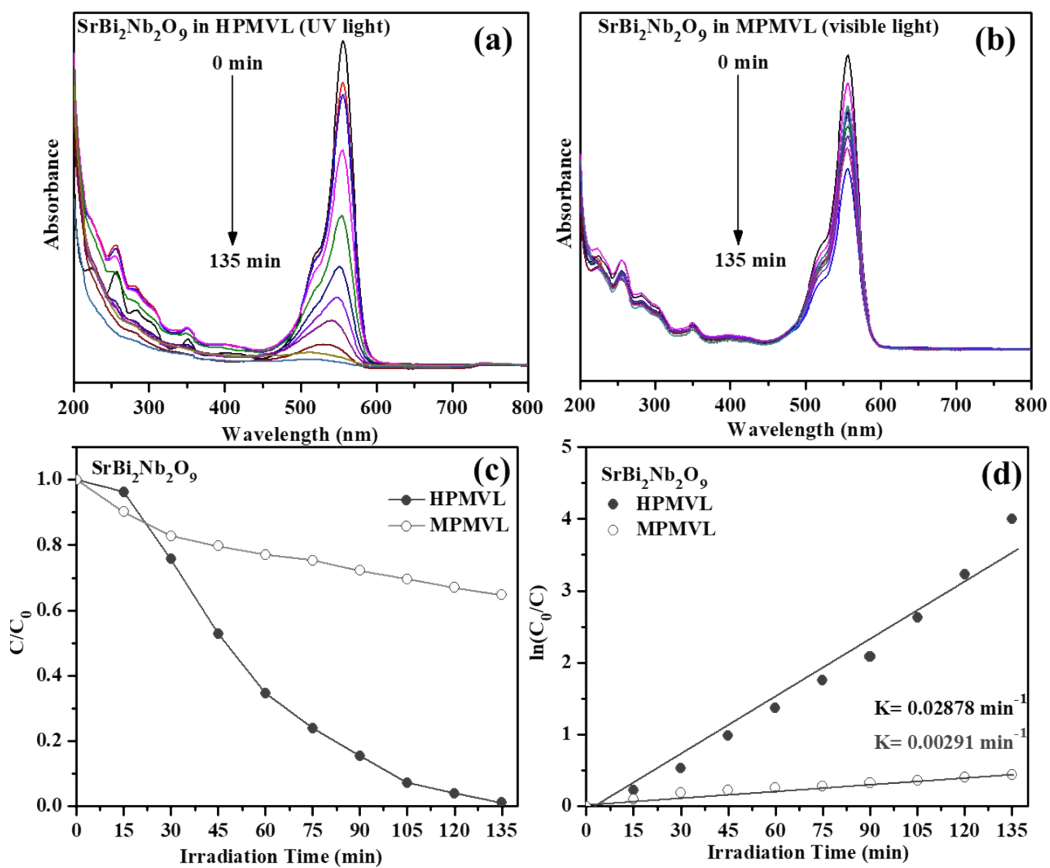


Fig. S9 RhB degradation over $\text{SrBi}_2\text{Nb}_2\text{O}_9$ at pH 2 under (a) high pressure mercury vapour lamp (HPMVL) and (b) medium pressure mercury vapour lamp (MPMVL). (c) C/C_0 and (d) $\ln(C_0/C)$ vs. time (min) plots for the same under HPMVL and MPMVL.

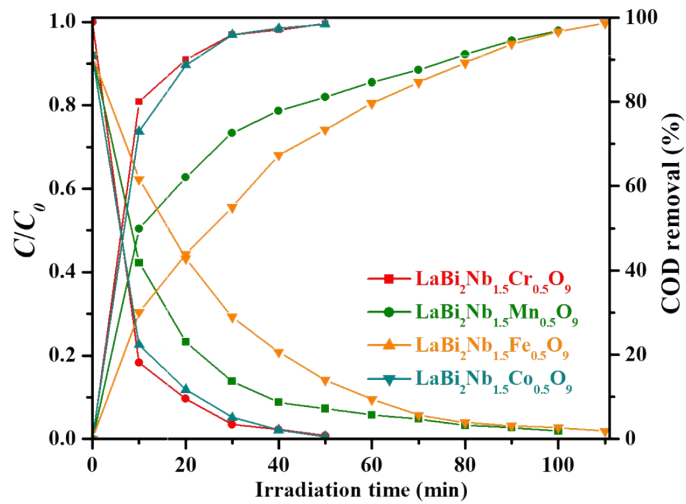


Fig. S10 C/C_0 and percentage COD removal with time for RhB degradation by $\text{LaBi}_2\text{Nb}_{1.5}\text{M}_{0.5}\text{O}_9$ ($\text{M} = \text{Cr}, \text{Mn}, \text{Fe}, \text{Co}$) at pH 2 under sunlight.

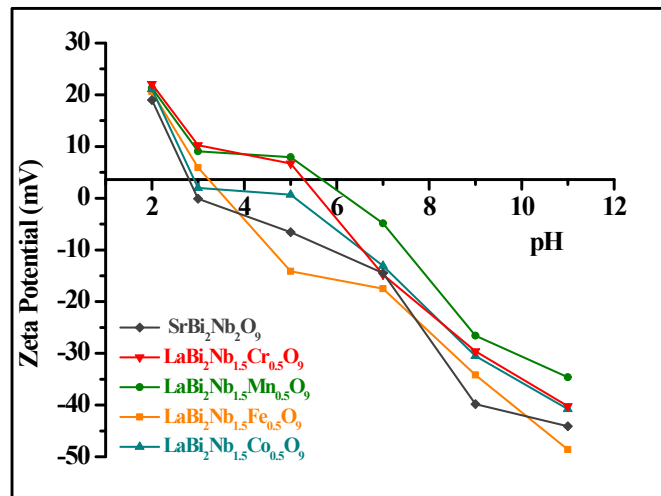


Fig. S11 ζ - potential of $\text{LaBi}_2\text{Nb}_{1.5}\text{M}_{0.5}\text{O}_9$ ($\text{M} = \text{Cr}, \text{Mn}, \text{Fe}, \text{Co}$) catalysts at different pH.

Table S4 BET surface area of $\text{LaBi}_2\text{Nb}_{1.5}\text{M}_{0.5}\text{O}_9$, ($\text{M} = \text{Cr}, \text{Mn}, \text{Fe}$ and Co) and $\text{SrBi}_2\text{Nb}_2\text{O}_9$

Catalyst	BET surface area (m ² /g)
$\text{SrBi}_2\text{Nb}_2\text{O}_9$	17.8
$\text{LaBi}_2\text{Nb}_{1.5}\text{Cr}_{0.5}\text{O}_9$	23.0
$\text{LaBi}_2\text{Nb}_{1.5}\text{Mn}_{0.5}\text{O}_9$	22.4
$\text{LaBi}_2\text{Nb}_{1.5}\text{Fe}_{0.5}\text{O}_9$	19.1
$\text{LaBi}_2\text{Nb}_{1.5}\text{Co}_{0.5}\text{O}_9$	16.0

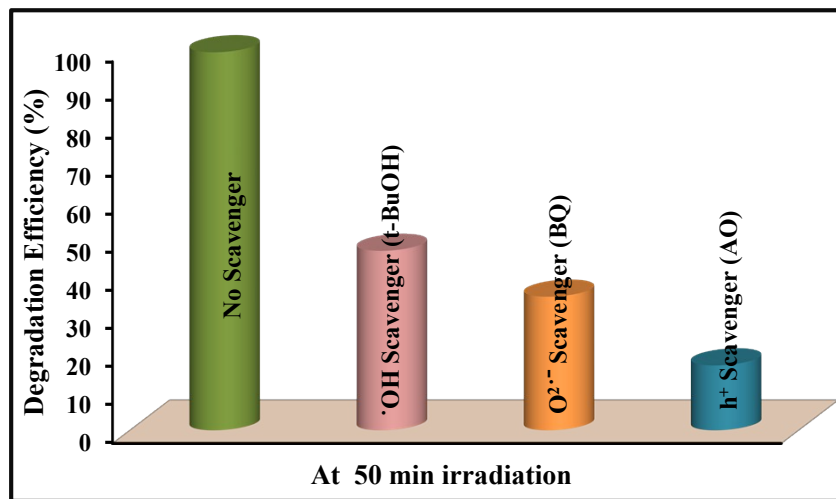


Fig. S12 Effect of different scavengers on the degradation of RhB over $\text{LaBi}_2\text{Nb}_{1.5}\text{Cr}_{0.5}\text{O}_9$ under sunlight-irradiation.

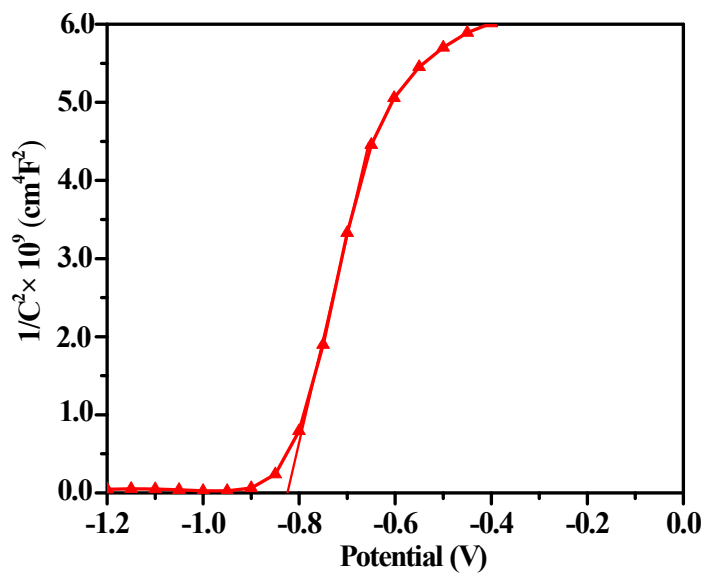


Fig. S13 Mott-Schottky plot for $\text{LaBi}_2\text{Nb}_{1.5}\text{Cr}_{0.5}\text{O}_9$ with Ag/AgCl as reference electrode and Pt as counter electrode in 0.1 M Na_2SO_4 (pH 2) at 50 Hz.